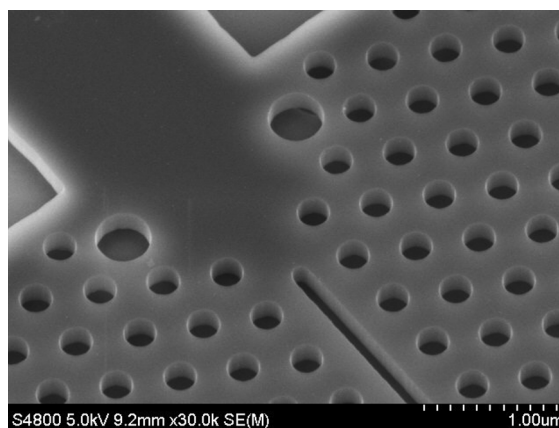


High Efficiency Interface for Coupling Into Slotted Photonic Crystal Waveguides

Volume 3, Number 2, April 2011

M. G. Scullion
T. F. Krauss
A. Di Falco



DOI: 10.1109/JPHOT.2011.2125785
1943-0655/\$26.00 ©2011 IEEE

High Efficiency Interface for Coupling Into Slotted Photonic Crystal Waveguides

M. G. Scullion, T. F. Krauss, and A. Di Falco

School of Physics and Astronomy, University of St. Andrews, KY16 9SS St. Andrews, U.K.

DOI: 10.1109/JPHOT.2011.2125785
1943-0655/\$26.00 ©2011 IEEE

Manuscript received February 4, 2011; revised March 2, 2011; accepted March 2, 2011. Date of publication March 22, 2011; date of current version March 25, 2011. A. Di Falco is supported by Engineering and Physical Sciences Research Council Career Acceleration Fellowship EP/I004602/1. Corresponding author: M. G. Scullion (e-mail: mgs32@st-andrews.ac.uk).

Abstract: We investigate the mechanism of coupling light into slotted photonic crystal waveguides. We identify two alternative approaches for improving the coupling efficiency, based on engineered mode dispersion and on resonant mechanisms. For the optimized geometry, we calculate a loss figure of 0.3 dB over 100-nm bandwidth per interface and demonstrate a corresponding experimental value of 1.5 dB over 78-nm bandwidth per interface.

Index Terms: Slotted photonic crystals, coupling, photonic crystals.

1. Introduction

Slotted photonic crystal (PhC) waveguides [1], [2] have recently attracted considerable interest as they combine the strong confinement of light in a low index medium such as air or polymers [3]–[6] with the strong confinement and dispersion engineering capability provided by PhC cavities and slow light structures. Slotted PhC geometries have already been used to demonstrate high Q cavities for applications such as chemical and gas sensing [7]–[11] and for polymer-based electrooptic modulators [12]–[14]. A common problem with these structures is the strong mismatch between the shape of the slotted mode and that of the incident ridge waveguide mode. Such shape discrepancy can be addressed with tapers, which is the typical solution used in regular slotted waveguides [15]. In the PhC case, however, this solution has yet to yield very high efficiency interfaces. The best theoretical coupling efficiency, to our knowledge, is $\sim - (1-2)$ dB per interface [12] obtained for higher order slot modes, which have more favorable properties from the coupling perspective but do not have the desired high field concentration in the slot. In order to improve the coupling efficiency, especially for the fundamental slot mode, the dispersive properties of the waveguides modes must be considered [2]. For example, if two modes have opposite gradients in their dispersion curves, coupling may occur into a backwards-propagating slot mode, which results in low transmission and strong Fabry–Perot fringes.

We have investigated two different coupling architectures, namely, a tapered and a resonant structure. Using plane wave (PW) calculations of photonic bands and Finite-Difference Time-Domain (FDTD) simulations, both in 2-D, we have established the conditions required for coupling between co-propagating modes. We then experimentally demonstrate the more efficient architecture, which is based on a resonant interface design.

2. Tapered Structure

Coupling into a standard slot waveguide is often achieved via a sharp taper in the ridge waveguide used to inject light into the slot. In the case of a slotted PhC, similar structures can be

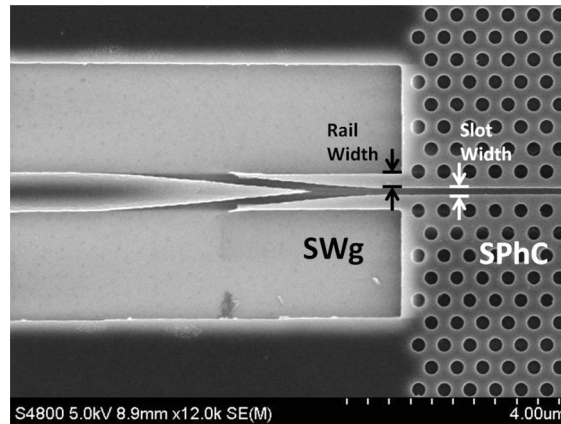


Fig. 1. SEM image of slotted photonic crystal coupler, with relevant geometrical parameters.

employed [12], whereby the input waveguide mode is first converted to a slot waveguide mode using a taper and then coupled into the PhC (see Fig. 1).

This simple approach works well for regular slotted waveguides, but it ignores the intricacies of the PhC environment, where the slope of the dispersion curve and, hence, the sign of the group velocity has to be taken into account; the modes' group velocity have to have the same sign to ensure that the energy flows in and out of the taper. In standard W1 PhC waveguides, this condition is met by matching the input waveguide and the PhC waveguide in the second Brillouin Zone (BZ) [16], where the group velocity of the two modes does have the same sign. The dispersion curve of the slotted PhC fundamental mode has the opposite sign from that of the standard W1 mode, however, so the input waveguide needs to be matched in the first BZ [2]. This requires the input waveguide to have a lower effective index, which is achieved by making the waveguide narrower, i.e., by reducing the rail width while keeping the slot width constant.

Fig. 2 illustrates the point; for a low effective index input waveguide [i.e., steep dispersion curve; see Fig. 2(c)], the matching condition is met in the first BZ, and the insertion loss is reasonable (3–5 dB between 1620 and 1720 nm, i.e., ≈ 2 dB per interface, similar to [12] [see Fig. 2(a)]. For a wider rail and, hence, higher effective index, input waveguide [i.e., shallower dispersion curve; see Fig. 2(d)], the dispersion curves meet in the second BZ, where the group index is of the opposite sign; as a result, the insertion loss, especially at the band-edge ($\lambda \approx 1600$ nm, $a/\lambda \approx 0.31$) is very high, on the order of 15 dB [see Fig. 2(b)]. While it is possible to match both the wave vectors and the direction of the group velocity by using a low effective index input waveguide, its physical realization is difficult. Mechanically stable and low loss slot rails of the required geometry are difficult to fabricate, especially when the substrate needs to be removed in order to create a PhC air-bridge; hence, no experimental measurements are provided here. In order to achieve high coupling efficiency in a system that can be fabricated more easily, we have therefore considered another solution, namely, a resonant coupler structure.

3. Resonant Structure

Several schemes exist for enhancing directional emission from standard PhCs [17]–[21]. These typically involve placing defects near the crystal edge, where interference effects between multiple beams produce a self-collimated beaming effect. It has recently been shown that resonant coupling can improve the insertion loss into a 2-D rod-based PhC waveguide [22] by increasing the size of the rods at the waveguide edge. Such larger rods create a resonance that preferentially couples with the desired waveguide mode. By adopting this principle to our system, we expect to demonstrate similar improvements in slotted PhC geometries, where relatively few coupling schemes exist [12], [23]. Unlike these schemes, we couple to the fundamental slot mode to take advantage of the high light confinement offered by this mode.

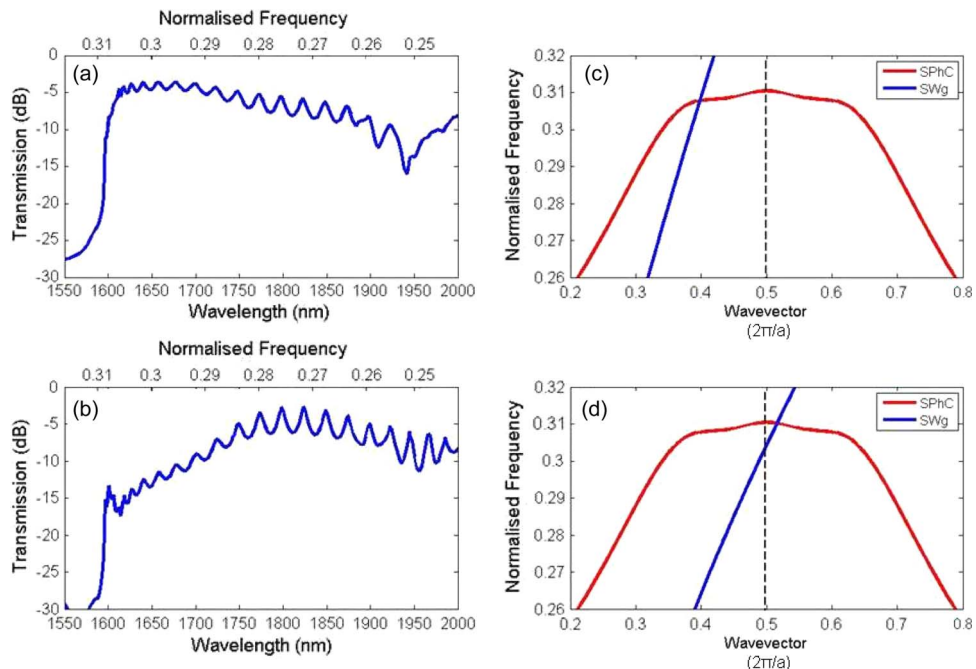


Fig. 2. Coupling between slotted waveguide and slotted PhC waveguide (2-D model including the 25- μm -long slot and both interfaces). Panels (a) and (b) show transmission curves for rail widths of 196 nm and 294 nm, respectively. Panels (c) and (d) show corresponding dispersion curves. Lattice constant used is $a = 490$ nm and slot width = 196 nm.

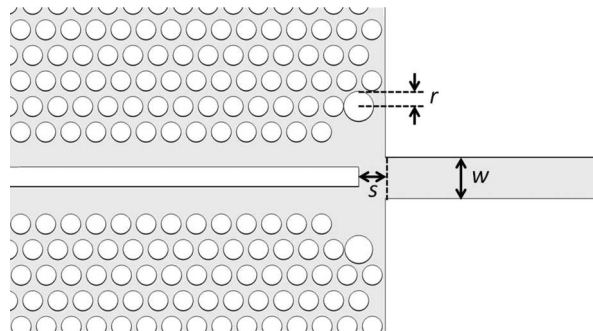


Fig. 3. Sketch of a resonant coupler structure highlighting the parameters that were optimized numerically.

Several geometrical parameters determine the resonant behavior of the resonant coupler, namely, the distance between the PhC edge and the beginning of the slot (s), the width of the access waveguide (w), and the radius of the holes (r).

A sketch of the geometry highlighting the different parameters is shown in Fig. 3. We simulate this structure using FDTD, choosing a period of 490 nm, hole radius 150 nm, slot width 180 nm, and effective refractive index 2.5. We excite the structures via a slab mode in the input access waveguide using a pulse centered on 1550 nm. Fig. 4 shows the transmission in normalized units (color coded) versus wavelength as we span the geometrical parameters s , r , and w . We note that the slot distance from the edge has the strongest impact on the transmission map.

The optimized structure has a broadband high transmission of average -0.6 dB over ($\Delta\lambda \approx 100$ nm [see Fig. 4(d)]), despite being based on a resonance (another coupling scheme based on resonance works for a bandwidth of ~ 35 nm [23]). The remaining ripple is due to the finite length of the slot, i.e., the device length, which indicates a finite remaining reflectivity at the

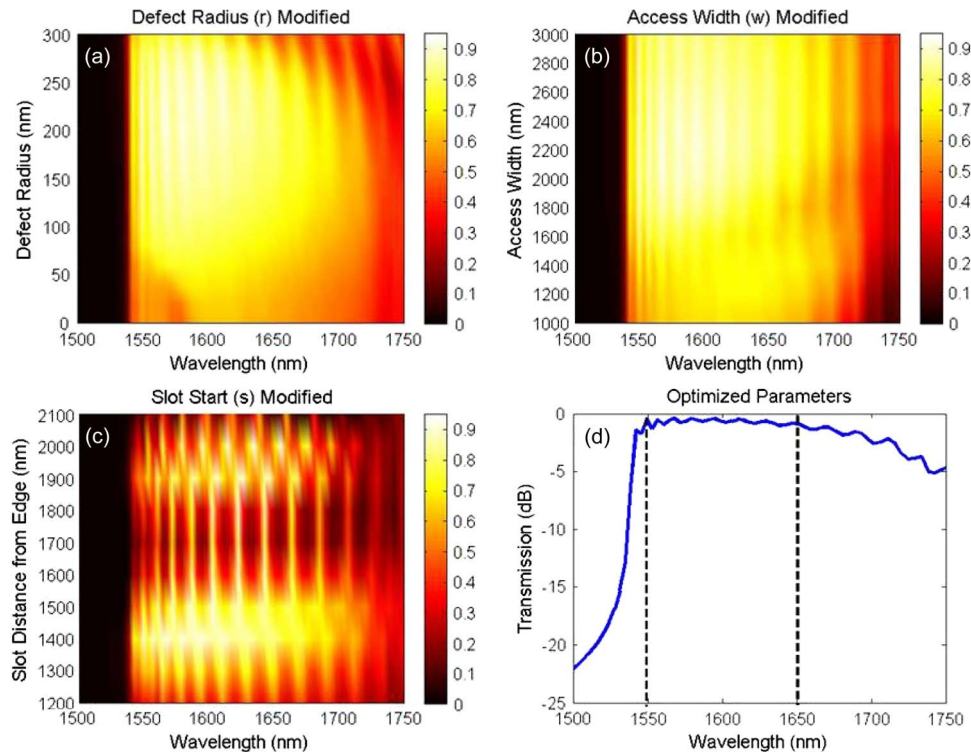


Fig. 4. Variation of SPhC linear transmission (2-D model including the 16.8- μm -long slot and both interfaces) with varying (a) defect radius, (b) access waveguide width, and (c) starting position of slot inside crystal. (d) Optimized log transmission using a defect radius of 220 nm, access width of 2200 nm, and slot start 1400 nm from the crystal edge. The average coupling efficiency per interface in the 1550–1650 nm wavelength window is -0.3 dB. In (a), note the low Q-factor of the resonance, which is key to the broadband operation of the coupler.

interface. Accordingly, we define a figure of merit based on the Fourier transform (FT) of the transmission spectrum. High transmission and low ripple is represented by a high ratio of the zero-order FT over the amplitude of the harmonics. The transmission spectrum of the device with the highest figure of merit is shown in Fig. 4(d). We expect the coupling geometry to require separate optimization for slow light engineered waveguides and here consider only standard SPhC waveguides; the general principle discussed here will apply for either type of waveguide, however.

4. Experimental Results

To verify the validity of the model experimentally, we fabricated a range of coupling structures in SOI material, of 220-nm top layer thickness, which is in line with the simulated parameters. We used electron-beam lithography, reactive ion etching (RIE), and HF undercutting to produce an air-bridge structure, as detailed in [1] and [2]. A scanning electron microscope (SEM) image of the final structure is shown in Fig. 5. A period of 490 nm, radius 145 nm, and slot width 150 nm were used in a 40-period-long SPhC. The distance of the slot from the edge of the crystal was varied in 100-nm steps, from 1300 to 1800 nm. The defect radius and access width were kept at 220 and 2200 nm, respectively, which is in line with their optimum values in simulations.

For the optical characterization, we used light from a broadband ASE source (1525–1620 nm) connected to a single mode fiber, polarization control (TE), and a $60\times$ objective lens for free-space optical injection. Waveguide input and output spots were observed using a $20\times$ objective and infrared camera from above, while the alignment was optimized using the voltage from a photodetector as a reference and was found to be stable. Fig. 6(a) shows the transmission versus wavelength and starting position of the slot, in analogy with the simulations shown in Fig. 4(c).

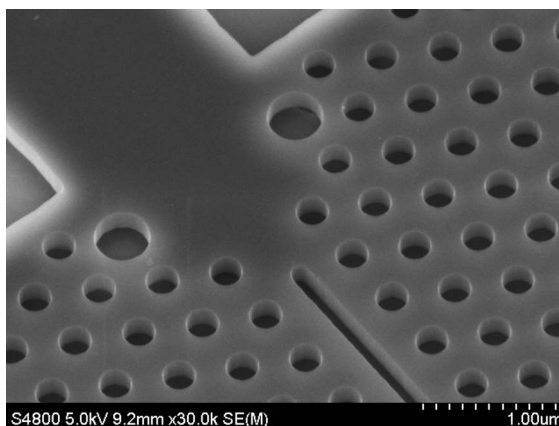


Fig. 5. SEM image of fabricated resonant coupler.

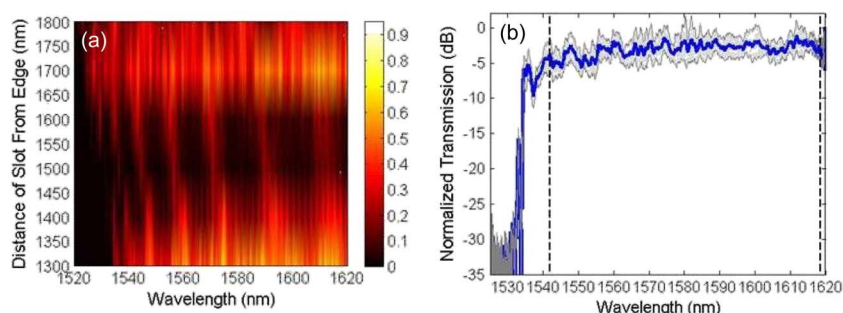


Fig. 6. Experimental results of transmission measurements for the complete device (a) variation of linear transmission with distance of slot edge inside crystal (b) cut of optimized \log transmission (distance of slot from edge of 1300 nm). Both graphs are normalized to nonslotted channel waveguides. Gray area shows standard deviation based on measurements of multiple reference waveguides.

Fig. 6(b) is extracted from Fig. 6(a) for a distance of the slot from the edge of 1300 nm. Comparison with Fig. 4 shows good agreement between experiment and theory, even though the simulation is only conducted in 2-D.

To isolate the contribution of the coupling region from other factors, we normalized the experimental transmission to that of a channel waveguide of the same length and constant width of $3 \mu\text{m}$ (which is identical to the access waveguide of the PhC). Fig 6(b) depicts the average transmission for the optimum geometry based on normalization to four reference waveguides, with the gray area depicting the standard deviation. From these measurements, we derive an average coupling loss of -3.0 ± 1.5 dB through the full device. Uncertainties arise from imperfections in the channel waveguides used for normalization. Both the numerical simulations and the experiments entail two interfaces, and therefore, the loss per interface is typically half that shown, and we derive an average value of -1.5 dB/interface over a 78-nm bandwidth, assuming negligible propagation losses, whose measurement will be addressed in future work.

5. Conclusion

We have considered the interface between a ridge waveguide and a slotted PhC waveguide and find that a simple taper structure is more difficult to realize in the slotted than in the corresponding nonslotted geometry, mainly because of the difficulty of matching the two waveguides in the same BZ. We then developed a coupler based on a resonant interface cavity. Optimization of multiple parameters (cavity size, access waveguide width, and slot position) yields a design with an average on-chip coupling loss of -0.3 dB over a 100-nm per interface. The high performance of the design

was verified by realizing the couplers experimentally, where we obtained -3.0 ± 1.5 dB over 78 nm through a device with two interfaces (-1.5 dB per interface). Uncertainties arise due to imperfections in the reference waveguides, but we note that our experimental value is well within the numerical predictions. The close agreement between the 2-D simulation and the 3-D experiment indicate that radiation losses are not the issue with these couplers but that mode-matching issues are the prime concern instead. It is also interesting to note that the resonator decouples the two sides of the interface and their corresponding dispersion curves, thus providing the required mode-matching. Furthermore, the resonant approach is surprisingly broadband, approaching 100 nm of bandwidth, due to the low Q of the resonance. Overall, the high performance of these couplers suggests that the interface into slotted PhC waveguides can be considered a solved problem.

References

- [1] A. Di Falco, L. O'Faolain, and T. F. Krauss, "Photonic crystal slotted slab waveguides," *Photonics Nanostruct. Fundam. Appl.*, vol. 6, no. 1, pp. 38–41, Apr. 2008.
- [2] A. Di Falco, L. O'Faolain, and T. F. Krauss, "Dispersion control and slow light in slotted photonic crystal waveguides," *Appl. Phys. Lett.*, vol. 92, no. 8, pp. 083501-1–083501-3, Feb. 2008.
- [3] V. R. Almeida, Q. Xu, C. A. Barrios, and M. Lipson, "Guiding and confining light in void nanostructure," *Opt. Lett.*, vol. 29, no. 11, pp. 1209–1211, Jun. 2004.
- [4] C. Koos, P. Vorreau, T. Vallaitis, P. Dumon, W. Bogaerts, R. Baets, B. Esembeson, I. Biaggio, T. Michinobu, F. Diederich, W. Freude, and J. Leuthold, "All-optical high-speed signal processing with silicon-organic hybrid slot waveguides," *Nat. Photonics*, vol. 3, no. 4, pp. 216–219, Apr. 2009.
- [5] A. Di Falco, C. Conti, and G. Assanto, "Quadratic phase matching in slot waveguides," *Opt. Lett.*, vol. 31, no. 21, pp. 3146–3148, Nov. 2006.
- [6] M. Hochberg, T. Baehr-Jones, G. Wang, J. Huang, P. Sullivan, L. Dalton, and A. Scherer, "Towards a millivolt optical modulator with nano-slot waveguides," *Opt. Exp.*, vol. 15, no. 13, pp. 8401–8410, Jun. 2007.
- [7] A. Di Falco, L. O'Faolain, and T. F. Krauss, "Chemical sensing in slotted photonic crystal heterostructure cavities," *Appl. Phys. Lett.*, vol. 94, no. 6, pp. 063 503-1–063 503-3, Feb. 2009.
- [8] T. Yamamoto, M. Notomi, H. Taniyama, E. Kuramochi, Y. Yoshikawa, Y. Torii, and T. Kuga, "Design of a high-Q air-slot cavity based on a width-modulated line-defect in a photonic crystal slab," *Opt. Exp.*, vol. 16, no. 18, pp. 13 809–13 817, Sep. 2008.
- [9] J. Gao, J. F. McMillan, M.-C. Wu, J. Zheng, S. Assefa, and C. W. Wong, "Demonstration of an air-slot mode-gap confined photonic crystal slab nanocavity with ultrasmall mode volumes," *Appl. Phys. Lett.*, vol. 96, no. 5, pp. 051123-1–051123-3, Feb. 2010.
- [10] S. H. Kwon, T. Sunner, M. Kamp, and A. Forchel, "Optimization of photonic crystal cavity for chemical sensing," *Opt. Exp.*, vol. 16, no. 16, pp. 11 709–11 717, Aug. 2008.
- [11] J. Jagerska, H. Zhang, Z. Diao, N. Le Thomas, and R. Houdre, "Refractive index sensing with an air-slot photonic crystal nanocavity," *Opt. Lett.*, vol. 35, no. 15, pp. 2523–2525, Aug. 2010.
- [12] J. M. Brosi, C. Koos, L. C. Andreani, M. Waldow, J. Leuthold, and W. Freude, "High-speed low-voltage electro-optic modulator with a polymer-infiltrated silicon photonic crystal waveguide," *Opt. Exp.*, vol. 16, no. 6, pp. 4177–4191, Mar. 2008.
- [13] J. H. Wulbern, J. Hampe, A. Petrov, M. Eich, J. Luo, A. K. Y. Jen, A. Di Falco, T. F. Krauss, and J. Bruns, "Electro-optic modulation in slotted resonant photonic crystal heterostructures," *Appl. Phys. Lett.*, vol. 94, no. 24, pp. 241107-1–241107-3, Jun. 2009.
- [14] X. Chen, Y. S. Chen, Y. Zhao, W. Jiang, and R. T. Chen, "Capacitor-embedded 0.54 pJ/bit silicon-slot photonic crystal waveguide modulator," *Opt. Lett.*, vol. 34, no. 5, pp. 602–604, Mar. 2009.
- [15] Z. Wang, N. Zhu, Y. Tang, L. Wosinski, D. Dai, and S. He, "Ultra-compact low-loss coupler between strip and slot waveguides," *Opt. Lett.*, vol. 34, no. 10, pp. 1498–1500, May. 2009.
- [16] H. Gersen, T. J. Karle, R. J. P. Engelen, W. Bogaerts, J. P. Korterik, N. F. van Hulst, T. F. Krauss, and L. Kuipers, "Real-space observation of ultraslow light in photonic crystal waveguides," *Phys. Rev. Lett.*, vol. 94, no. 7, p. 073903, Feb. 2005.
- [17] E. Moreno, F. J. Garcia-Vidal, and L. Martin-Moreno, "Enhanced transmission and beaming of light via photonic crystal surface modes," *Phys. Rev. B*, vol. 69, no. 12, p. 121 402(R), Mar. 2004.
- [18] S. Morrison and Y. S. Kivshar, "Engineering of directional emission from photonic-crystal waveguides," *Appl. Phys. Lett.*, vol. 86, no. 8, pp. 081110-1–081110-3, Feb. 2005.
- [19] W. R. Frei, D. A. Tortorelli, and H. T. Johnson, "Topology optimization of a photonic crystal waveguide termination to maximize directional emission," *Appl. Phys. Lett.*, vol. 86, no. 11, pp. 111114-1–111114-3, Mar. 2005.
- [20] C.-C. Chen, T. Pertsch, R. Iliew, F. Lederer, and A. Tunnermann, "Directional emission from photonic crystal waveguides," *Opt. Exp.*, vol. 14, no. 6, pp. 2423–2428, Mar. 2006.
- [21] H. Kurt, "Theoretical study of directional emission enhancement from photonic crystal waveguides with tapered exits," *IEEE Photon. Technol. Lett.*, vol. 20, no. 20, pp. 1682–1684, Oct. 2008.
- [22] J. Bauer and S. John, "Broadband optical coupling between microstructured fibers and photonic band gap circuits: Two-dimensional paradigms," *Phys. Rev. A*, vol. 77, no. 1, pp. 013819-1–013819-14, Jan. 2008.
- [23] X. Chen, W. Jiang, J. Chen, L. Gu, and R. T. Chen, "20 dB-enhanced coupling to slot photonic crystal waveguide using multimode interference coupler," *Appl. Phys. Lett.*, vol. 91, no. 9, pp. 091111-1–091111-3, Aug. 2007.